DOI: 10.1002/chem.200800835

Cationic Metal–Corrole Complexes: Design, Synthesis, and Properties of Guanine-Quadruplex Stabilizers

Boqiao Fu, Dan Zhang, Xiaocheng Weng, Ming Zhang, Heng Ma, Yuzhi Ma, and Xiang Zhou*[a]

Abstract: A series of pyridinium and quaternary ammonium copper corroles has been designed and synthesized. All new compounds have been fully characterized by NMR spectroscopy, high-resolution mass spectrometry, UV/Vis spectrscopy, and elemental analysis. Biochemical studies have indicated that all of these corrole derivatives can stabilize G-quadruplex structures, with corrole **4** being the most effective according to the results of circular dichroism (CD) melting experiments, polymerase chain reaction (PCR) stop assays, and surface plasmon resonance (SPR) experiments. Moreover, both corroles **3** and **4** tend to induce the human telomeric sequence to form hybrid G-quadruplex structures, whereas corroles **8** and **9** are more inclined to induce the human telomeric sequence to form antiparallel G-quadruplex structures.

Keywords: chelation · corroles · DNA · guanine · quadruplexes

Introduction

Corroles are tetrapyrrolic macrocycles, akin to porphyrins, but with one less carbon atom in their outer periphery and one additional NH proton in their inner core. The two types of macrocycles have the same 18 π-electron conjugated system.[1] It has been reported that the NH proton in the inner core of corroles is strongly acidic, whereas the NH proton in the porphyrins is weakly basic.[2] Corroles are trianionic ligands that stabilize metal ions in unusually high oxidation states, for example copper(III). Corroles can stabilize high-valent metals, whereas porphyrins cannot because the strong σ donation, which in turn greatly increases the energy of the d orbitals of the metal, is a more dominant effect than the high energy of the corrole π system relative to that of the porphyrins.[3]

Telomeres consist of tandem repeats of guanine-rich TTAGGG sequences at the terminal of all chromosomes. These sequences can cap the ends of chromosomes and protect them from deleterious processes during replication steps. Further investigation has indicated that these repeats may fold into intramolecular G-quadruplex structures.[4] The enzyme telomerase, which mediates the maintenance of telomeres, is overexpressed in tumor cells. When the 3′ end of the telomere folds into a G-quaruplex, the activities of telomerase are inhibited, thus killing the tumor cells without destroying the normal cells. It has been reported that telomeres can form G-quadruplex structures in the presence of Na^+ or K^+ ions.[5]

Thus, devising ways of stabilizing G-quadruplex structures has become a key strategy in the design of antitumor agents. Recently, many groups have synthesized series of G-quadruplex stabilizers, which may block the extension of telomeres by telomerase, thereby confering antitumor activities with potential medicinal applications.[6] The porphyrin family was one of the first that was identified as G-quadruplex stabilizers. Cationic porphyrins, such as TMPyP4, display good inhibitory activities toward telomerase.[6e,f] Gross and co-workers were the first to synthesize cationic corroles and find that they can interact with DNA,[7] and we reported that some cationic corroles are capable of stabilizing G-quadruplex structures and inhibiting the activity of telomerase.[8]

To study the structure–activity relationships of corroles, we attached pyridinium, piperidine, dimethylamino, and amide moieties to the corrole skeleton because these functional groups have shown a good affinity for DNA.[9–16] Metals also play important roles in biological systems, and metal complexes can influence the activities of telomer-

[a] B. Fu,[+] D. Zhang,[+] Dr. X. Weng, M. Zhang, H. Ma, Y. Ma, Prof. X. Zhou
College of Chemistry and Molecular Sciences
Wuhan University, Hubei
Wuhan 430072 (China)
Fax: (+86) 27-8733-6380
E-mail: xzhou@whu.edu.cn

[+] Both authors contributed equally to this study.

Supporting information for this article is available on the WWW under http://dx.doi.org/10.1002/chem.200800835.

ase.[17] Some studies have reported special chemical properties of metallated corroles. Metal ions with high-oxidation states in the core of the corrole may strengthen the interaction between the corroles and G-quadruplexes. X-ray crystallographic studies of corrolatocopper and -manganese complexes show that they are typically saddle-type, which are very similar to a plane.[7,18] These structures make cationic corroles prone to matching the G-quartet, which could strengthen the interaction of the molecular ligand and G-quadruplex. In view of these points, some metal ions with high-oxidation states, such as copper(II) and manganese(II), were inserted into corroles to form trivalent complexes.

However, there are few reports on the interaction between the metal–corrole complexes and G-quadruplexes. Considering the specific structures of metalated corroles,[7,18] we anticipated these compounds would show some interesting properties through interaction with G-quadruplex DNA. Thus, a metal–corrole complex may possibly play an important role in replacing one of the metal ions that is normally coordinated in and at the ends of the central ion channel of the quadruplex.[19]

Herein, we report some new findings concerning the synthesis and biochemical studies of cationic corrole derivatives. Biochemical studies include a polymerase chain reaction (PCR) stop assay, circular dichroism (CD) studies, CD melting assays, surface plasmon resonance (SPR) experiments, and UV titration experiments. The results have indicated that the synthesized cationic corrole derivatives are capable of stabilizing G-quadruplex structures.

Results and Discussion

Synthesis and physicochemical characterization: We recently reported that some water-soluble free cationic corrole derivatives showed good inhibitory activity toward telomerase and induced the formation of a G-quadruplex structure.[8] These compounds also showed good selectivities for G-quadruplex DNA over double-stranded DNA (dsDNA). We have now designed and synthesized more functionalized corrole derivatives to investigate their structure–activity relationships further.

The strategy of synthesis of these metal-chelating corroles, in which the metal centers were inserted into the corroles and then different groups were attached, was based on the stronger acidity of the inner hydrogen atoms. This property makes these corroles very active under basic conditions and the inner nitrogen atom is easily alkylated, thus leading to reactions that produce more by-products. It is very difficult to use an aldehyde with a basic group to synthesize the corroles directly, partially as a result of the ready protonation of the basic group, thus making the aldehyde prone to reacting with pyrrole to form porphyrins instead of corroles.

The corrole derivatives were synthesized in metal-assisted reactions. For the synthesis of corroles **8**, **9**, and **12**–**15**, the key step was the alkylation of phenol in the presence of a strong base.[20] To avoid alkylation of the inner nitrogen atom of the corrole, a metal-protected core is necessary. Furthermore, it has been reported that manganese and copper derivatives are good at stabilizing corroles and have good biological activities.[21] Therefore, manganese and copper were chosen as our studied metals.

In our initial synthesis of cationic corroles, we mixed 4-pyridine corrole with metal acetates in pyridine and obtained complexes **1** and **2** (Scheme 1). Methylation of corroles **1** and **2** with methyl iodide in THF/CH_3OH then afforded the water-soluble pyridinium corroles **3** and **4** in good yield. The copper or manganese centers in the complexes became Cu^{III} or Mn^{III}, which has been detailed in many reports.[22] The free 5,10,15-tris(4-aminophenyl)corrole and 5,10,15-tris(4-pyridyl)corrole are neutral, whereas these two corroles are basic on metal chelation because the strongly acidic hydrogen atoms in the inner core are replaced by the metal centers. The structures of the free corroles have the stronger coplane character rather than the saddle-type structure of the metal–corroles.

Quaternary ammonium corroles were synthesized according to the procedures shown in Scheme 2. Using 5,10,15-tris(4-hydroxyphenyl)corrole as a starting material, we formed the corresponding copper complex by treatment with copper(II) acetate in pyridine at room temperature. Further alkylation of the phenol groups with alkyl chlorides in the presence of K_2CO_3 furnished corroles **6** and **7**. Finally, methylation of **6** and **7** with methyl iodide gave the quaternary ammonium corroles **8** and **9** in good yield. The low

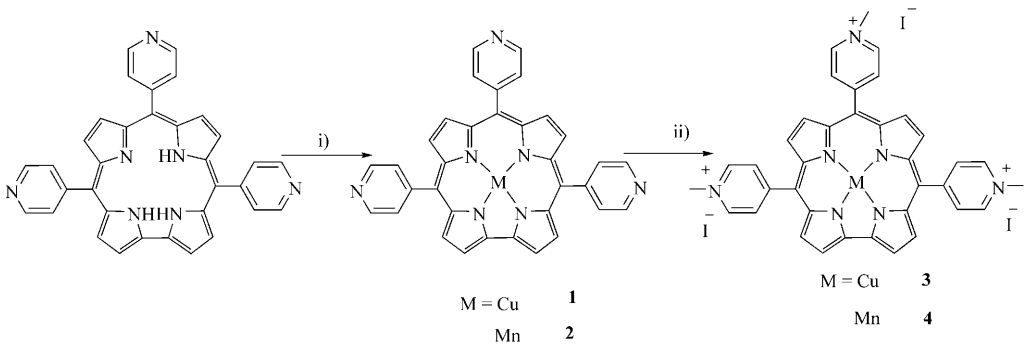

Scheme 1. i) $Cu(Ac)_2$, pyridine, 30 min, RT; $Mn(Ac)_2$, pyridine, 30 min, 60 °C; ii) THF/CH_3OH, 40 °C, 12 h.

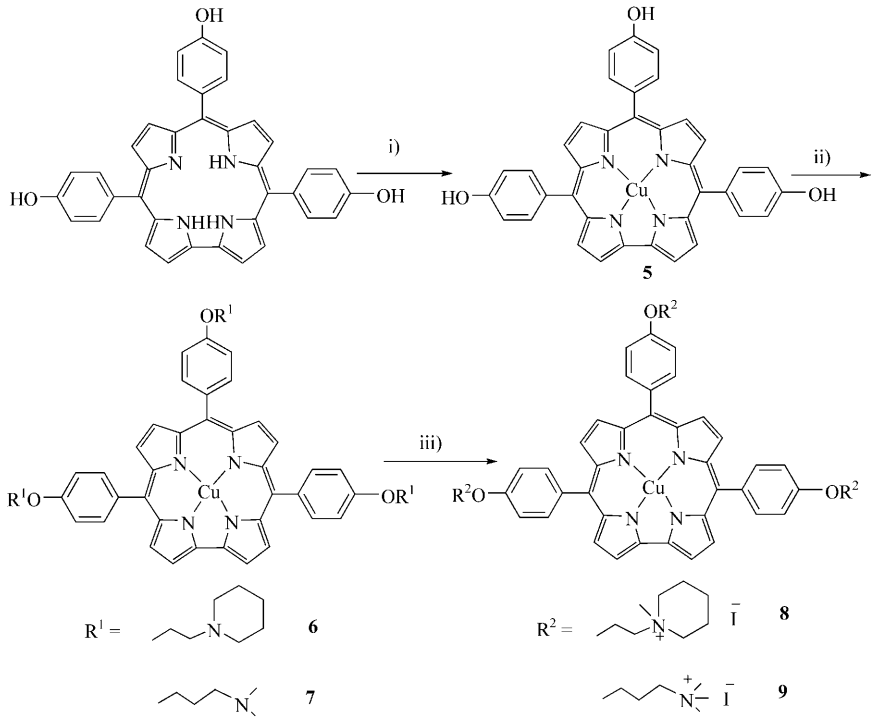

Scheme 2. i) $Cu(AC)_2$, pyridine, RT, 30 min; ii) 1-(2-chloroethyl)piperidine hydrochloride or 3-chloro-*N*,*N*-dimethylpropan-1-amine hydrochloride, K_2CO_3, 60 °C, 72 h; iii) CH_2Cl_2, CH_3I, 40 °C.

yields of **6** and **7** might be attributed to the high-oxidation state of the copper center, strong inductive effect of which leads to low electron density at the periphery. The electron density on the oxygen atom of the hydroxy group was thereby significantly lowered, thus rendering it only weakly nucleophilic.

Compounds **12–15** were synthesized from 5,10,15-tris(4-aminophenyl)corrole (Scheme 3). Treatment with copper(II) acetate afforded 5,10,15-tris(4-aminophenyl)corrolate copper (**10**) in good yield. The important intermediate **11** was prepared by mixing **10** and 4-(chloromethyl)benzoyl chloride at room temperature. Finally, the quaternary ammonium copper corrole derivatives **12–15** were obtained in good yield by treating **11** with tri-

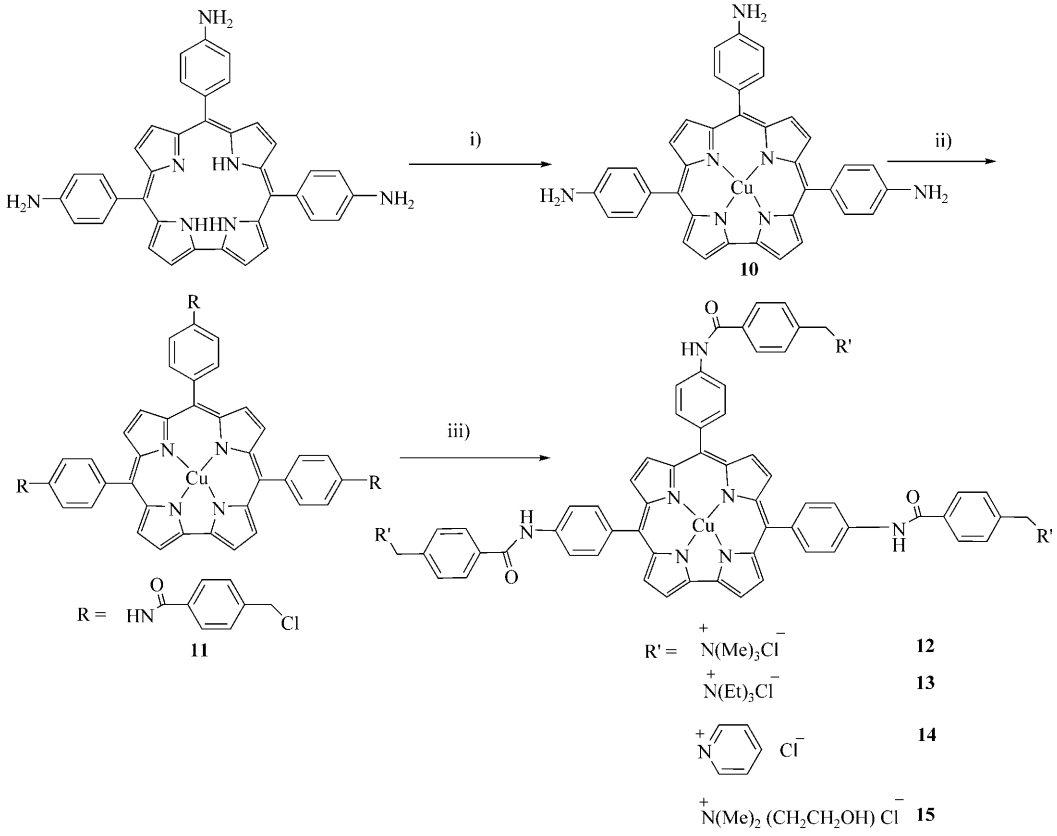

Scheme 3. i) $Cu(Ac)_2$, pyridine, 30 min, RT; ii) 4-(chloromethyl)benzoyl chloride, NEt_3, THF, RT, 2 h; iii) THF, 33% trimethylamine, alcohol solution, RT, 12 h; NEt_3, reflux 13 h; pyridine, reflux 14 h; 2-(dimethylamino)ethanol, reflux 15 h.

methylamine, triethylamine, and pyridine, respectively. All new compounds were fully characterized by NMR spectroscopy, high-resolution mass spectrometry, UV/Vis spectroscopy, and elemental analysis.

Stabilizing the G-quadruplex structure in the telomeric sequence and c-MYC region G-quadruplexes sequence by PCR stop assay:[23,26] Nondenaturing polyacrylamide gel electrophoresis (PAGE) was used to ascertain whether the corrole derivatives bonded to the test oligomer 21G (5′-GGGTTAGGGTTAGGGTTAGGG-3′) and stabilized the G-quadruplex structure.[24,25] The sequences of the tested oligonucleotides (21G and 21Gmu) and the corresponding complementary sequence (Rev 21G), which is a complementary oligonucleotide that partially hybridized to the last G repeat of the test oligonucleotide used here, are presented in Figure 1. Taking the result of the PCR stop assay of corrole **13** as an example, we can find that the inhibitory effect of **13** is enhanced dramatically as the concentration is increased from 1.0 to 15.0 μM (see gel (a) shown in Figure 2a with the corresponding dose–response curve). The IC_{50} value, which indicates the concentration of **13** required to achieve 50% inhibition of the reaction, was found to be 7.07 μM (the values shown in Table 1 were obtained at least from three repeated experiments)

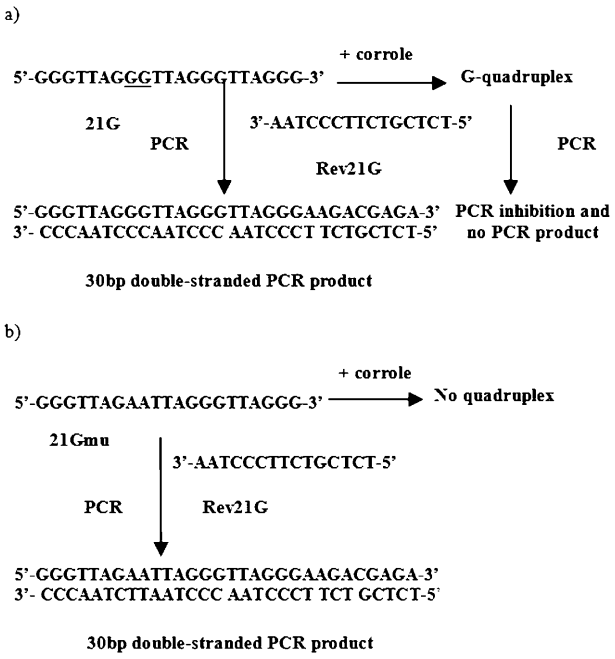

Figure 1. a) The principle behind the PCR stop assay: The test oligomer (21G or 21Gmu) was amplified with a complementary oligomer (Rev21G) overlapping the last six bases TTAGGG. A final 30-base-pair (bp) double-stranded PCR product was available through a successfully carried out PCR process in the absence of corroles. On the addition of a corrole, 21G could be induced into and stabilized as a G-quadruplex structure. At this time, no PCR product will be obtained because of the PCR inhibition or because Taq polymerase extension is inhibited. b) If the two underlined bases GG in 21G were replaced by adenine (A), a mutative sequence 21Gmu could not form a G-quadruplex structure in the presence of G ligands.

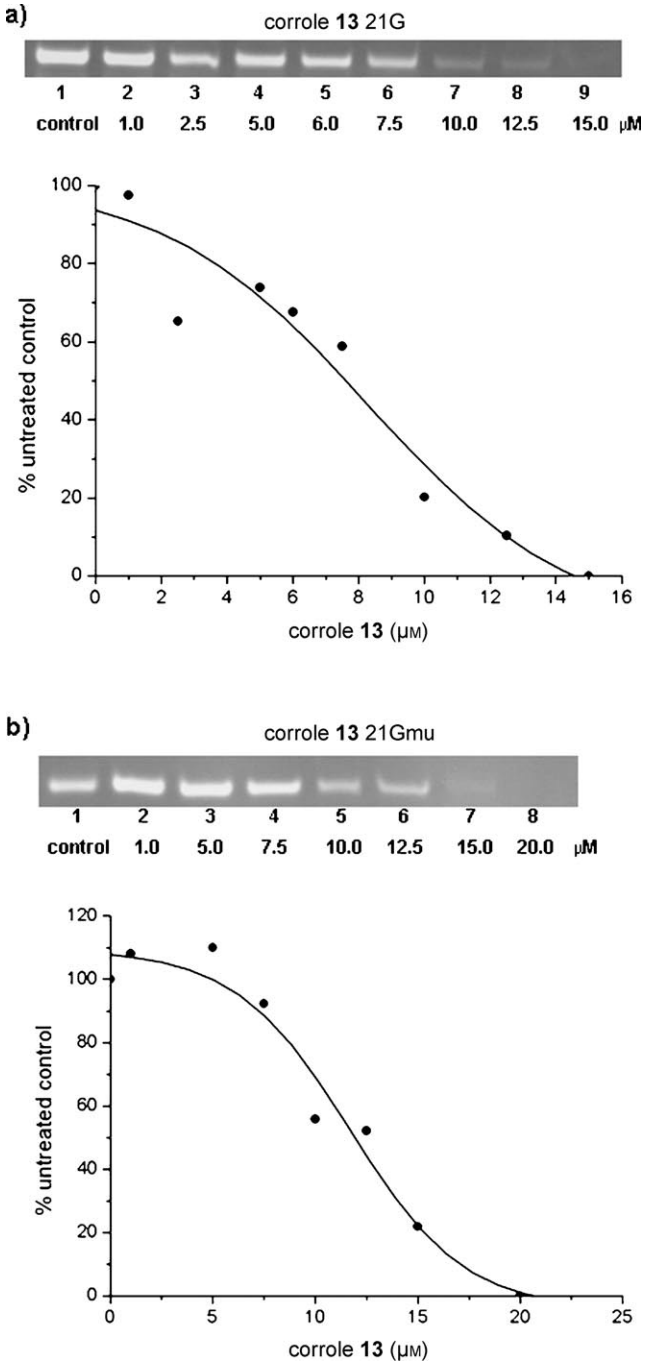

Figure 2. Effect of corrole **13** on the formation of the PCR stop assay with G-quadruplex forming 21G oligomer (gel a) or on the parellel assay with the corresponding mutated oligomer 21Gmu (gel b). Increasing concentrations of **13** were added to the G-quadruplex forming 21G or 21Gmu oligomers. The assay used a buffer containing 10 mM K^+ and 1.5 mM Mg^{2+} ions. The quantification of the final 30-bp double-stranded PCR product is shown by the lighteness of fluorescence determined by using Chemilmager 5500 (Alpha Innotech, San Leandro, CA) and are displayed by dose–response curves.

A nonspecific PCR inhibition experiment using a mutated oligomer 21Gmu (5′-GGGTTA GAATTA GGGTTA GGG-3′) instead of the oligomer 21G, which could not form the G-quaduplex structure, was performed (Figure 1b). The gel

Table 1. Effects of the corrole derivatives on telomeric quadruplexes and C-Myc measured by the PCR stop assay.

Compound	IC_{50} [μM]		Telo selectivity
	21G	21Gmu	
3	3.51±2.14	7.09±1.70	2.02
4	2.37±1.01	6.46±1.92	2.72
8	7.70±0.40	10.95±2.95	1.42
9	12.35±1.74	14.03±1.62	1.14
12	10.87±0.14	>30.00	>2.76
13	7.07±0.47	11.62±0.64	1.64
14	5.99±2.27	6.28±1.43	1.05
15	6.30±3.30	5.19±2.07	0.82
Compound	IC_{50} [μM]		C-Myc selectivity
	Pu27	Pu27mu	
3	2.74±0.40	4.19±2.68	1.53
4	1.52±0.31	3.23±1.70	2.13
8	15.34±1.97	4.52±0.44	0.29
9	9.59±2.28	9.67±0.27	1.01
12	7.62±2.57	4.44±1.72	0.58
13	10.31±2.51	7.43±0.92	0.72
14	5.39±0.78	5.12±0.41	0.95
15	4.88±0.40	3.48±1.33	0.71

in Figure 2b with the corresponding dose–response curve shows the inhibitory properties of **13** to a PCR process with similar concentration gradients. Compared with the corresponding concentration of **13** in the gel in Figure 2a, it is clear that whereas **13** totally stabilizes the G-quadruplex formation of the 21G oligomer at 15 μM, it cannot totally inhibit the extension of Taq polymerase or the PCR process. The IC_{50} value of this reaction between **13** and the 21Gmu oligomer was 11.62 μM relative to the previous IC_{50} value of 7.07 μM; thus, we can conclude that corrrole **13** has a good selectivity for the human telomeric sequence.

The results of the PCR stop assay of the eight cationic corroles **3**, **4**, **8**, **9**, and **12**–**15** toward the human telomeric sequence 21G and mutated sequence 21Gmu are presented in Table 1. Relative to other corrrole derivatives, corrole **4** displayed the highest selectivity of 2.72. This outcome clearly indicates that corrole **4**, which is modified with pyridine at the *meso* position of the corrole plane and chelated with a manganese ion, is better than other corroles in this assay because it can both stabilize a G-quadruplex at a lower concentration and has better selectivity.

Another sequence Pu27 (5′-TGGGGAGGGTGGGGAGGGTGGGGAAGG-3′), which existed in the NHE III_1 element of the C-Myc gene promoter[26,27] and could form a parallel G-quadruplex structure, was chosen to replace the oligomer 21G to further demonstrate the conclusion presented above by utilizing the same principle. Similarly, oligomer Pu27mu (5′-TGGGGAGGGTGGAAAGGGTGGGGAAGG-3′) was chosen to substitute 21Gmu. Detailed results obtained for these corroles are summarized in Table 1; all compounds were found to be active at the micromolar range both in the Telo and C-Myc systems.

Among the eight corroles, **4** was found to be the most active in this assay, with an IC_{50} value of 1.52 μM in the C-Myc system (IC_{50}=2.37 μM in the Telo system). Additionally, **4** also possessed the best selectivity of the two systems, which can be attributed in a large degree to its special structure. We suggest that an electron-withdrawing group, such as the pyridinium moiety in **3** and **4**, decreased the electron density of the corrole ring, thus leading to interaction with the more electron-rich G-quaduplex DNA. Alternatively, a trivalent manganese–corrole complex could strengthen the interaction of the molecular ligand and G-quadruplex and present a relatively higher affinity toward the G-quadruplex because of its higher electron deficiency and favorable shape.[28]

Structure induction or transition of the G-quadruplex in the presence of corrole derivatives tested by CD spectroscopy: CD spectroscopy was used to determine the structure induction and structure transition of the G-quadruplex in the presence of cationic corrole derivatives. It has been reported that the human telomeric $d(T_2AG_3)_4$ sequence forms a typical antiparallel G-quadruplex structure in the presence of Na^+ ions and has a positive band near λ=295 nm and a negative band at λ=265 nm in CD spectra.[29] On the other hand, in the presence of K^+ ions, there is a small positive band at λ=265 nm, a negative band close to λ=240 nm, and a stronger positive peak at λ=295 nm, which may be characteristic of a hybrid of parallel/antiparallel G-quadruplex structures.[30]

Figure 3 shows CD spectra of the structures obtained by adding different concentrations of corrole **4** to the human telomeric sequence Telo24 in the absence of a high concentration of free univalent metal ions.[6b,31] The CD profile of single-strand Telo24 (5′-TTAGGGTTAGGGTTAGGGTTAGGG-3′) shows a positive band at λ=257 nm attributable to the absorbance of individual bases. On adding increasing amounts of **4**, there is a sharp decrease in the band at λ=257 nm accompanied by a sharp increase in the band around λ=295 nm, thus showing the formation of hybrid of parallel/antiparallel G-quadruplex structures.[6b,8]

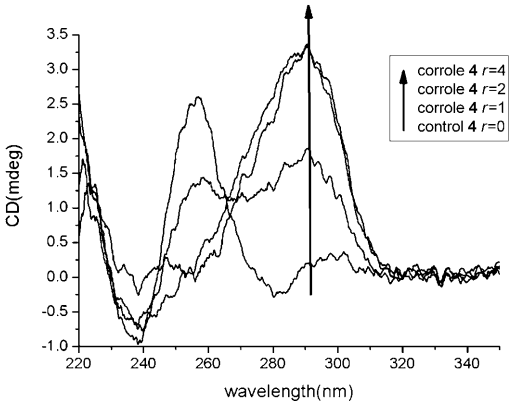

Figure 3. CD spectroscopic titration of the G-quadruplex $(T_2AG_3)_4$ with corrole **4** in the absence of 100 mM NaCl. Arrows from bottom to up indicated increments in *r* values from 0 to 4. (r=corrole **4**/$(T_2AG_3)_4$).

From other CD spectra (see Figure S1 in the Supporting Information), we could conclude that both **3** and **4** tend to induce the human telomeric sequence to form hybrid G-quadruplex structures, whereas corroles **8** and **9** tend to induce the human telomeric sequence to form antiparallel G-quadruplex structures. However, the other corroles, such as **12**–**15**, do not induce the same sequences in any G-quadruplex structure formation. Therefore, this finding suggests that pyridinium and piperidinium quaternary ammonium substituents at the *meso* positions might interact with the loops and grooves of a G-quadruplex,[32] whereas phenyl amide substituents at the *meso* positions do not have this ability to interact with DNA.

Table 2. Values of T_m and ΔT_m for the antiparallel G-quadruplex of the human telomeric sequence stabilized by corrole derivatives.

	Compound								
	control	**3**	**4**	**8**	**9**	**12**	**13**	**14**	**15**
T_m [°C]	37.1	54.5	58.4	62.8	63.8	42.8	45.6	46.1	46.1
ΔT_m [°C]		17.4	21.3	25.7	26.7	5.7	8.5	9.0	9.0

Thermodynamic stability of G-quadruplex structures in the presence of corrole derivatives: The binding capacities of the corrole derivatives to the G-quadruplex structure, thus reflecting the degree of stabilization, were studied by CD melting experiments.[8] CD spectroscopy was also used to measure the thermodynamic stability profile of the G4C oligomer (sequence 5′-CATGGTGGTTTGGGTTAGGGTTAGGGTTAGGGTTACCAC-3′) incubated with the corrole derivatives in the presence of Na^+ ions. In these experiments, thermal CD transitions were monitored at $\lambda =$ 295 nm, which is diagnostic of the antiparallel G-quadruplex structure in the human telomeric sequence.[8]

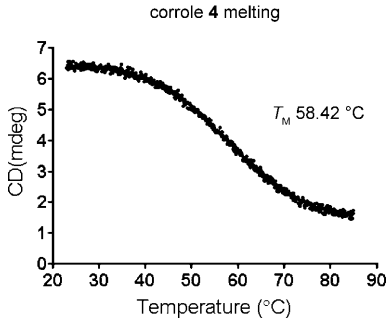

Figure 4. CD melting curve of 12.5 μM DNA oligonucleotide (G4C) and corrole **4** in 100 mM NaCl at pH 7.4, 10 mM Tris–HCl, and 1 mM EDTA buffer. The CD spectra were monitored at $\lambda = 295$ nm. The concentration ratio of corrole/DNA (r) is 5:1.

Figure 4 shows the melting curve of **4** in the presence of 100 mM Na^+ ions, 10 mM 2-amino-2-(hydroxymethyl)-1,3-propanediol hydrochloride (Tris—HCl), and 1 mM ethylenediaminetetraacetic acid (EDTA) at pH 7.4. The concentration of **4** was five times greater than the G4C oligomer. Table 2 displays the ΔT_m values of the eight corroles ($R = 5$) (see Figure S2 in the Supporting Information for the melting curves). All the corrole derivatives possess the ability to stabilize the G-quadruplex structure in the presence of Na^+ ions. Among the eight cationic corroles, the ΔT_m values of **3**, **4**, **8**, and **9** are higher than those of the other cationic corroles. As explained before, four of them interact well with the G-quadruplex, thus suggesting that **3**, **4**, **8**, and **9** are able to stabilize the G-quadruplex DNA well.

The ΔT_m values of **8** and **9** are 25.7 and 26.7 °C, respectively, which suggests that these corroles are more able to stabilize the G-quadruplex structure. However, this outcome seem to conflict with the results of the PCR stop assay, which suggested that **3** and **4** are more able to stabilize the G-quadruplex structure. We assume that these conflicting results are a result of the different buffers used in the two experimental systems. In the PCR stop assay, the samples contained 10 mM K^+ and 1.5 mM Mg^{2+} ions, which could induce the Telo sequence to form a parallel/antiparallel G-quadruplex structure.[6b] Under these conditions, **3** and **4** may favor this structure because **3** and **4** could induce a hybrid of parallel/antiparallel G-quadruplexes, thus leading to improved stabilization of the G-quadruplex. In the CD melting experiment, the tested samples included 100 mM Na^+ ions that induced the Telo sequence to form an antiparallel G-quadruplex structure, which may be favorable for **8** and **9** because they could induce the Telo sequence to form the same structure.

Selectivities of corroles comparing the G-quadruplex to double-stranded DNA (dsDNA) tested by SPR: The binding abilities and constants of corroles **3**, **4**, **8**, and **9** to the G-quadruplex were quantitatively determined by using SPR (Table 3). The experimental data are shown in Table 3 (see Figure S3 in the Supporting Information for sensorgrams), and we can take the ratio of K_A(G4)/K_B(dsDNA) to evaluate the selectivities of the corroles.[6b,28,31] We found that **3** and **4** had better selectivities than other corroles by comparing the four ratios of K_A(G4)/K_B dsDNA). Corrole **4** was the most selective because its binding constant to the G4 sequence was about 64 times greater than binding to the dsDNA sequence. Relative to the 4-pyridinium corrole ligand in the absence of copper or manganese, the selectivities of **3** or **4** to the G-quadruplex were sligtly decreased.[8] It is probable that the formation of copper or manganese corroles did not result in suitable shapes to interact with the G-quadruplex DNA compared with the 4-pyridinium corrole. Further SRA experiments on this series of compounds are under investigation.

Binding modes of corroles/G-quadruplex and corroles/calf thymus DNA (CT-DNA) by UV/Vis titration: To find the binding modes of the corroles to G-quadruplex DNA and dsDNA, we measured their maximium absorbance in the

Table 3. Equilibrium binding constants determined by SPR and rate constants for quadruplex interactions, determined from BIAcore analysis of 1:1 binding with mass-transfer fitting.

Compound	DNA	k_a[a]	k_d[a]	K_A[b]	K_D[c]	K_A(G4)/K_A(dsDNA)
3	G4	2.16×10^{4}	2.26×10^{-3}	9.53×10^{6}	1.05×10^{-7}	49.4
	dsDNA	4.13×10^{2}	2.14×10^{-3}	1.93×10^{5}	5.18×10^{-6}	
4	G4	4.34×10^{3}	2.24×10^{-3}	1.94×10^{6}	5.17×10^{-7}	63.6
	dsDNA	7.75×10^{1}	2.54×10^{-3}	3.05×10^{4}	3.28×10^{-5}	
8	G4	3.70×10^{2}	1.33×10^{-3}	2.78×10^{5}	3.60×10^{-6}	1.7
	dsDNA	3.05×10^{2}	1.86×10^{-3}	1.64×10^{5}	6.10×10^{-6}	
9	G4	1.80×10^{2}	6.24×10^{-3}	2.88×10^{4}	3.47×10^{-5}	1.2
	dsDNA	1.61×10^{2}	6.84×10^{-3}	2.35×10^{4}	4.26×10^{-5}	

[a] Kinetic constants (k_a and k_d are the corresponding association and dissociation rate constants) determined from BIAcore analysis by using 1:1 Langmuir global fitting of 240-s association and 240 s disassociation. [b] Determined from k_a/k_d. [c] Determined from k_d/k_a.

Conclusion

A series of new cationic copper and manganese corroles has been designed and synthesized by using different strategies. Biochemical studies indicate that all of the eight cationic corroles **3**, **4**, **8**, **9**, and **12–15** can stablize G-quadruplex structures. Furthermore, corrole derivatives **3** and **4** can induce the hybrid formation of a parallel/antiparallel G-quadruplex structure of the human telomeric sequence and corroles **8** and **9** could induce the formation of an antiparallel G-quadruplex structure, as examined by CD spectroscopy.

Among these corroles, manganese–corrole **4** with pyridinium substituents at the *meso* position of the corrole unit exerts a better stabilization effect toward the G-quadruplex structure. The strong electron-withdrawing groups (i.e., pyridinium substituents on the periphery of corrole and the trivalent manganese) decrease the electron density of the corrole ring, thus allowing ready interaction with the electron-rich guanine G-quadruplex. SPR data suggested that corroles **3** and **4** showed good selectivity between dsDNA and G-quadruplexes.

Interestingly, these corroles could also stabilize the G-quadruplex structure of Pu27 of NHE III_1, as determined by PCR stop assays. The experimental results suggested that corrole **4** had the best ability to stabilize the G-quadruplex structure of Pu27 of NHE III_1 among all the tested corroles. This series of corroles has potential in antitumor applications.

presence of G4 DNA or duplex DNA by UV/Vis titration (see Figures S4 and S5 in the Supporting Information). We found that the absorbance was red shifted by less than 8 nm and that the hypochromicity was between 10 and 35% for the interaction between the corroles and G4 DNA (Table 4). It is suggested that corroles **8**, **9**, and **12–15** have different binding modes compared with **3** and **4**,[33] because of the increased bulkiness of the G4 DNA relative to corroles.

Table 4. Effect of G4A on the absorption maximum of the Soret band for corroles.

Compound	λ_{max} [nm]	G4A		Red shift [nm]
		λ_{max} [nm]	H [%][a]	
3	437	453	37	16
4	500	520	37	20
8	423	436	26	13
9	409	436	29	27
12	417	421	13	4
13	424	427	22	3
14	419	423	16	4
15	419	423	17	4

[a] H=[Abs free−Abs corrole (bound)]/Abs free; Abs free is the absorbance of each corrole at the concentration of 2.5 μM without any DNA; Abs corrole (bound) is the absorbance of the fully bound corroles as measured at the Soret maxium of free corrole.

For the interaction between corroles and dsDNA (i.e., CT-DNA), we found that all the corroles, except **3**, might have the same binding mode with CT-DNA because the absorbance was red shifted by less than 8 nm and the hypochromicity was between 10 and 35% in the UV/Vis spectra (see Table 5 and Figure S5 in the Supporting Information).[34] We explained that corrole **3** with pyridinium arms has a planar structure, as determined by X-ray crystallographic analysis,[22b] and can intercalate into CT-DNA. Corrole **4** has axis coordination to the manganese complex, and this steric effect prohibits it from intercalating with CT-DNA.[7] Other corroles with steric side arm groups might not interact with CT-DNA in the same way as **4**.

Table 5. Effect of CT-DNA on the absorption maximium of the Soret band for corroles.

Compound	λ_{max} [nm]	CT-DNA		Red shift [nm]
		λ_{max} [nm]	H [%][a]	
3	435	462	37	27
4	500	505	22	5
8	423	424	39	1
9	421	424	23	3
12	419	425	12	6
13	424	429	23	5
14	420	426	15	6
15	420	426	11	6

[a] H=[Abs free−Abs corrole (bound)]/Abs free; Abs free is the absorbance of each corrole at the concentration of 2.5 μM without any DNA; Abs corrole (bound) is the absorbance of the fully bound corroles as measured at the Soret maxium of free corrole.

Experimental Section

Physical methods: The NMR spectra were recorded on a Varian Mercury VX-300 MHz spectrometer operating at 300 MHz for ^{1}H NMR. Chemical shifts in the ^{1}H NMR spectra are reported in ppm relative to the residual hydrogen atoms in the deuterated solvents: $\delta = 2.50$ and 7.25 ppm for $[D_6]$DMSO and $CDCl_3$, respectively. The coupling constants J are reported in Hz. Mass-spectroscopic analysis was performed on a VG ZAB-HS instrument. UV/Vis spectra were collected with Beijing Purkinje General Instrument TU-1900 spectrophotometer. The elemental analysis was performed on a Elementary Vario ElIII CHNSO machine.

Materials: *N*,*N*-Dimethylformamide (DMF) and pyrrole were distilled over CaH_2 before use. Absolute anhydrous THF was distilled over Na. 1-(2-Chloroethyl)piperidine hydrochloride was obtained from Alfa Aesar. The other reagents and solvents were bought from Sinopharm Chemical Reagent Co., Ltd.

Synthetic methods: The synthetic details of the preparation 5,10,15-tris(4-hydroxylphenyl)corrole, 5,10,15-tris(4-aminophenyl)corrole, and 5,10,15-tris(4-pyridyl)corrole are provided in our previous report.[8]

5,10,15-Tris(4-pyridyl)corrolatocopper(III) (1): A solution of 5,10,15-tris(4-pyridyl)corrole (95 mg, 0.18 mmol) and cupric acetate hydrate (538 mg, 5.4 mmol) in pyridine (20 mL) was stirred at room temperature for 30 min. The solvent was evaporated and the crude solid was purified by chromatography on alumina (200–300 mesh) by elution with $CH_3COOEt/CH_3OH = 10:1$ and 5:1 to collect the first yellow–green fraction. After removal of the solvents, the solid was recrystallized from THF/petroleum ether (1:5). Compound **1** was obtained as a black solid in 43% yield (46 mg, 0.078 mmol). ^{1}H NMR (300 MHz, $CDCl_3$, 25°C, TMS): $\delta = 7.13$ (d, $^3J(H,H) = 3.6$ Hz, 4H; pyridine H), 7.27 (s, 2H; pyridine H), 7.47–7.56 (m, 7H; β-pyrrole H and pyridine H), 7.90 (s, 2H; β-pyrrole H), 8.74 ppm (s, 5H; β-pyrrole H); ^{13}C NMR (75 MHz, $CDCl_3$, 25°C, TMS): $\delta = 122.78$, 125.21, 130.27, 133.03, 144.87, 146.42, 150, 150.6 ppm; UV/Vis (THF): λ_{max} ($\varepsilon \times 10^{-3}$ L mol^{-1} cm^{-1}) = 407 (106.5), 542 (9.5), 617 (6.1) nm; HRMS (ESI): m/z: calcd for $C_{34}H_{20}N_7Cu+H$: 590.1149; found: 590.1145 [$M+H^+$]; elemental analysis (%) calcd for $C_{34}H_{20}N_7Cu\cdot H_2O$: C 67.15, H 3.65, N 16.12; found: C 67.14, H 3.41, N 16.16.

5,10,15-Tris(4-pyridyl)corrolatomanganese(III) (2): A solution of 5,10,15-tris(4-pyridyl)corrole (100 mg, 0.19 mmol) and manganese acetate tetrahydrate (463 mg, 1.9 mmol) in pyridine (20 mL) was heated by using an oil bath at 60°C for 30 min. The solvent was evaporated and the resulting solid was isolated by chromatography on alumina (200–300 mesh) by gradient elution with CH_3COOEt/CH_3OH (10:1, 5:1, 2:1) to collect the first yellow–green fraction. After evaporation of the solvents, the crude product was recrystallized from THF/petroleum ether (1:5). Compound **2** was obtained as a green solid in 31% yield (34 mg, 0.059 mmol). ^{1}H NMR (300 MHz, $[D_6]$DMSO/$[D_4]CH_3OH$ (1:1), 25°C, TMS): $\delta = 8.87$ (br s, 5H; β-pyrrole H), 7.00–7.80 ppm (br s, 15H; β-pyrrole H and pyridine H); UV/Vis (THF): λ_{max} ($\varepsilon \times 10^{-3}$ L mol^{-1} cm^{-1}) = 403 (55.4), 438 (63.95), 494 (44.5), 554 (12.55), 583 (15.55), 648 (21.25) nm; HRMS (ESI): m/z: calcd for $C_{34}H_{20}N_7Mn+H$: 582.1233; found: 582.1234 [$M+H^+$] (100%); elemental analysis (%) calcd for $C_{34}H_{20}N_7Mn\cdot H_2O$: C 68.91, H 3.70, N 16.35; found: C 68.95, H 3.91, N 16.59.

5,10,15-Tris(*N*-methyl-4-pyridyl)corrolatocopper(III) (3): A solution of 5,10,15-tris(4-pyridyl)corrolatocopper (45 mg, 0.076 mmol) and CH_3I (10 mL, 0.16 mmol) in a mixture of acetone (20 mL) and methanol (2 mL) was heated at 40°C overnight. The solvent was evaporated and the crude product was recystallized from methanol/petroleum ether (1:2). Compound **3** was obtained as a black solid in 52% yield (43 mg, 0.042 mmol). ^{1}H NMR (300 MHz, $[D_6]$DMSO, 25°C, TMS): $\delta = 4.52$ (s, 9H; CH_3), 9.14 ppm (br s, 20H; β-pyrrole H and pyridine H); UV/Vis (CH_3OH): λ_{max} ($\varepsilon \times 10^{-3}$ L mol^{-1} cm^{-1}) = 427 (16.7), 506 (35.76), 665 (10.52) nm; HRMS (ESI): m/z: calcd for ($C_{37}H_{29}I_3CuN_7-3I$)/3: 211.3927; found: 211.3929 [M^+-3I]/3; elemental analysis (%) calcd for $C_{37}H_{29}I_3CuN_7\cdot 3H_2O$: C 41.53, H 3.30, N 9.16; found: C41.36, H3.52, N9.16.

5,10,15-Tris(*N*-methyl-4-pyridyl)corrolatomanganese(III) (4): Compound **4** was obtained by using the same procedures described for **3**. The starting materials was 5,10,15-tris(4-pyridyl)corrolatomanganese (26 mg, 0.045 mmol) and **4** was obtained in 73% yield (33 mg, 0.033 mmol). ^{1}H NMR (300 MHz, $[D_7]$DMF/CD_3OD (1:1), 25°C, TMS): $\delta = 4.56$ (s, 9H, CH_3), 8.00–8.40 (m, 9H; β-pyrrole H and pyridine H), 8.95–9.20 ppm (m, 11H; β-pyrrole H and pyridine H); UV/Vis (CH_3OH): λ_{max} ($\varepsilon \times 10^{-3}$ L mol^{-1} cm^{-1}) = 427 (16.4), 506 (35.76), 665 (10.52) nm; HRMS (ESI): m/z: calcd for ($C_{37}H_{29}I_3MnN_7-3I$)/3: 208.7288; found: 208.7285 [M^+-3I]/3; elemental analysis (%) calcd for $C_{37}H_{29}I_3MnN_7\cdot 3H_2O$: C 41.87, H 3.32, N 9.24; found: C 41.77, H 3.14, N 8.82.

5,10,15-Tris(4-phenol)corrolatocopper(III) (5): Compound **5** was obtained by using the same procedure described for **1.** The starting materials were 5,10,15-tris(4-hydroxylphenyl)corrole (460 mg, 0.8 mmol) and cupric acetate hydrate (4.60 g, 23 mmol). The resulting solid was isolated by chromatography on silical gel (200—300 mesh) and eluted with ethyl acetate/cyclohexane (1:2). The first brown fraction was collected. After evaporatation of the solvent, the crude product was recrystallized from acetone/petroleum ether (1:5). Compound **5** was obtained as a brown solid in 59% yield (300 mg, 0.47 mmol). ^{1}H NMR (300 MHz, $[D_6]$DMSO, 25°C, TMS): $\delta = 6.84$–6.92 (m, 6H; Ph–H), 7.22 (d, $^3J(H,H) = 8.1$ Hz; 4H; Ph–H), 7.38 (d, $^3J(H,H) = 7.8$ Hz, 2H; Ph–H), 7.51 (m, 6H; β-pyrrole H), 7.83 (s, 2H; β-pyrrole H), 9.93 (s, 1H; OH), 9.99 ppm (s, 2H; OH); ^{13}C NMR (75 MHz, $[D_6]$DMSO, 25°C, TMS): $\delta = 115.67$, 116.01, 121.47, 126.99, 129.49, 130.28, 132.20, 131.11, 143.93, 145.08, 150.34, 152.54, 158.58, 158.95 ppm; UV/Vis (acetone): λ_{max} ($\varepsilon \times 10^{-3}$ L mol^{-1} cm^{-1}) = 431 (104.7), 637 (6.2), 547 (12.8) nm; HRMS (ESI): m/z: calcd for $C_{37}H_{23}CuN_4O_3$: 634.1066; found: 634.1052; elemental analysis (%) calcd for $C_{37}H_{23}CuN_4O_3\cdot H_2O$: C 68.04, H 3.86, N 8.58; found: C 67.61, H 3.82, N 8.38.

5,10,15-Tris(4-{[1-(2-ethyl)piperidine]oxy}phenyl)corrolatocopper(III) (6): A suspension of **5** (300 mg, 0.47 mmol), 1-(2-chloroethyl)piperidine hydrochloride (533 mg, 2.84 mmol), and K_2CO_3 (685 mg, 4.96 mmol) in dry DMF (50 mL) was stirred under N_2 and heated by using an oil bath at 60°C for 72 h. The solvent was evaporated under reduced pressure. The residue was dissolved in dichloromethane (300 mL) and washed with water. The organic layer was evaporated under reduced pressure. The resulting solid was isolated by chromatography on alumina (200—300 mesh) with ethyl acetate/methanol (100:1). The first fraction was collected and the solvent was evaporated. Further purification was carried out by recrystallization from methanol/dichloromethane (5:1). Compound **6** was obtained as a red–brown solid in 27% yield (123 mg, 0.127 mmol). ^{1}H NMR (300 MHz, $CDCl_3$, 25°C, TMS): $\delta = 1.42$ (s, 6H; piperidine H), 1.59 (s, 12H; piperidine H), 2.50 (s, 12H; piperidine H), 2.79 (s, 6H; NCH_2), 4.15 (d, $^3J(H,H) = 4.5$ Hz, 6H; OCH_2), 6.91–6.97 (m, 6H; Ph-H), 7.29 (d, $^3J(H,H) = 7.5$ Hz; 4H, Ph-H), 7.57 (d, $^3J(H,H) = 7.5$ Hz, 2H; Ph-H), 7.63–7.68 (m, 6H; β-pyrrole H), 7.79 ppm (s, 2H; β-pyrrole H); ^{13}C NMR (75 MHz, $CDCl_3$, 25°C, TMS): $\delta = 24.43$, 26.19, 55.32, 58.19, 66.29, 114.32, 114.54, 121.31, 129.52, 131.78, 132.34, 133.02, 144.29, 145.54, 150.77, 159.29, 159.53 ppm; UV/Vis (CH_2Cl_2): λ_{max} ($\varepsilon \times 10^{-3}$ L mol^{-1} cm^{-1}) = 435 (99), 548 (10.4), 627 (5) nm; HRMS (ESI): m/z: calcd for $C_{58}H_{62}N_7CuO_3+H^+$: 968.4283; found: 968.4276 [$M+H^+$]; elemental analysis (%) calcd for $C_{58}H_{62}N_7CuO_3\cdot H_2O$: C 70.60, H 6.54, N 9.94; found: C71.05, H 6.40, N 10.15.

5,10,15-Tris{4-[(3-dimethylaminopropionylamino)oxy]phenyl}corrolatocopper(III) (7): A suspension of **5** (91 mg, 0.47 mmol), 3-chloro-*N*,*N*-dimethylpropan-1-amine hydrochloride (136 mg, 0.86 mmol), and K_2CO_3 (208 mg, 1.5 mmol) in dry DMF (50 mL) was stirred under N_2 and heated by using oil bath at 60°C for 72 h. The solvent was evaporated under reduced pressure. The residue was dissolved in dichloromethane (300 mL) and washed with water. The organic layer was evaporated under reduced pressure. The resulting solid was isolated by chromatography on alumina (200–300 mesh) with ethyl acetate/methanol (50:3). The first fraction was collected and the solvent was evaporated. The crude product was recrystallized from petroleum ether. Compound **7** was obtained as a red–brown solid in 20% yield (26 mg, 0.029 mmol). ^{1}H NMR (300 MHz, $CDCl_3$, 25°C, TMS): $\delta = 2.04$ (s, 6H; CH_2), 2.30 (s, 18H; NCH_3), 2.52 (s, 6H; NCH_2), 4.13 (s, 6H; OCH_2), 6.96–7.03 (m, 6H; Ph-H), 7.35 (d, $^3J(H,H) =$

6.6 Hz, 4H; Ph-H), 7.64–7.75 (m, 8H; β-pyrrole H and pyridine H), 7.87 ppm (s, 2H; β-pyrrole H); ^{13}C NMR (75 MHz, $CDCl_3$, 25 °C, TMS): δ = 27.77, 45.73, 56.65, 66.54, 114.26, 114.49, 121.29, 127.00, 129.46, 131.80, 133.02, 144.29, 145.57, 150.77, 159.72 ppm; UV/Vis (CH_2Cl_2): λ_{max} ($\varepsilon \times 10^{-3}$ L mol^{-1} cm^{-1}) = 434 (79.75), 541 (7.75), 636 (2.4) nm; HRMS (ESI): *m/z*: calcd for $C_{52}H_{26}CuN_7O_3$+H: 890.3813; found: 890.3825 $[M+H]^+$; elemental analysis (%) calcd for $C_{52}H_{26}CuN_7O_3 \cdot H_2O$: C 68.74, H 6.43, N 10.79; found: C 68.79, H 6.32, N 10.87.

5,10,15-Tris(4-{[1-(2-ethyl)-*N*-methyl-piperidine]oxy}phenyl)corrolatocopper(III) (8): A solution of **6** (50 mg, 0.052 mmol) and CH_3I (10 mL, 0.16 mmol) in dichloromethane (30 mL) was stirred under N_2 and heated by using an oil bath at 40 °C for 24 h. The solvent was evaporated and the resulting solid was washed with CH_2Cl_2 and Et_2O in turn. Compound **8** was obtained as a brown solid in 82% yield (59 mg, 0.04 mmol). ^{1}H NMR (300 MHz, [D$_6$]DMSO, 25 °C, TMS): δ = 1.60 (s, 6H; piperidine H), 1.89 (s, 12H; piperidine H), 3.21 (s, 9H; NCH_3), 3.51 (d, ^3J(H,H) = 1.5 Hz, 12H; piperidine H), 3.91 (s, 6H; NCH_2), 4.61(s, 6H; OCH_2), 7.18–7.24 (m, 6H; Ph-H), 7.31(s, 2H; Ph-H), 7.41 (s, 2H; Ph-H), 7.66 (s, 2H; Ph-H and β-pyrrole H), 7.76 (d, ^3J(H,H) = 8.1 Hz, 4H; β-pyrrole H), 8.16 ppm (s, 2H; β-pyrrole H); ^{13}C NMR (75 MHz, [D$_6$]DMSO, 25 °C, TMS): δ = 19.27, 20.47, 47.87, 60.83, 61.22, 114.57, 114.77, 122.12, 131.83, 133.20, 143.08, 149.23, 157.91, 158.17 ppm ; UV/Vis (CH_3OH): λ_{max} ($\varepsilon \times 10^{-3}$ L mol^{-1} cm^{-1}) = 424 (112.7), 530 (9.95), 627 (5) nm; HRMS (ESI): *m/z*: calcd for $C_{61}H_{71}CuN_7O_3I_3$; found: 337.4960 $[M^+-3I]/3$ (100%), 569.6955 $[M^+-2I]/2$ (14%), 337.4971 $[M^+-3I]/3$, 569.6979 $[M^+-2I]/2$; elemental analysis (%) calcd for $C_{61}H_{71}CuN_7O_3I_3 \cdot H_2O$: C 51.87, H 5.21, N 6.94; found: C 52.05, H 5.21, N 7.03.

5,10,15-Tris{4-[(3-trimethylaminopropionylamino)oxy]phenyl}corrolatocopper(III) (9): A solution of **7** (30 mg, 0.034 mmol) and CH_3I (10 mL, 0.16 mmol) in dichloromethane (40 mL) was stirred under N_2 and heated by using an oil bath at 40 °C for 24 h . The solvent was evaporated and the resulting solid was washed with CH_2Cl_2 and Et_2O in turn. Compound **9** was obtained as a brown solid in 90% yield (40 mg, 0.03 mmol). ^{1}H NMR(300 MHz, [D$_6$]DMSO, 25 °C, TMS): δ = 2.28 (s, 6H; CH_2), 3.15 (s, 27H; NCH_3), 3.56 (s, 6H; NCH_2), 4.21 (s, 6H; OCH_2), 7.17 (d, ^3J-(H,H) = 8.1 Hz, 6H; Ph-H), 7.31 (s, 2H; Ph-H), 7.40 (s, 2H; Ph-H), 7.67 (s, 3H; Ph-H and β-pyrrole H), 7.74 (d, ^3J(H,H) = 7.2 Hz, 5H; β-pyrrole H), 8.14 ppm (s, 2H; β-pyrrole H); ^{13}C NMR (75 MHz, [D$_6$]DMSO, 25 °C, TMS): δ = 23.38, 53.14, 63.78, 65.76, 115.19, 115.40, 132.80, 159.60, 159.85 ppm; UV/Vis (CH_3OH): λ_{max} ($\varepsilon \times 10^{-3}$ L mol^{-1} cm^{-1}) = 427 (91.35), 544 (8.35), 634 (3.9) nm; HRMS (ESI): *m/z*: calcd for $[C_{55}H_{65}CuI_3N_7O_3-3I]/3$: 311.4819; found: 311.4806 $[M^+-3I]/3$; elemental analysis (%) calcd for $C_{55}H_{65}CuI_3N_7O_3 \cdot 2H_2O$: C 48.84, H 5.14, N 7.25; found: C 48.41, H 5.35, N 6.98.

5,10,15-Tris(4-aminophenyl)corrolatocopper(III) (10): A solution of 5,10,15-tris(4-aminophenyl)corrole (524 mg, 0.92 mmol) and cupric acetate hydrate (5.24 g, 26.3 mmol) in pyridine (50 mL) was stirred at room temperature for 30 min. The solvent was evaporated and the resulting solid was isolated by chromatography on alumina (200–300 mesh) with THF/methanol (10:1). The second brown fraction was collected. After removal of the solvents under reduced pressure, the solid was recrystallized from THF/petroleum ether. Compound **10** was obtained as a black–brown solid in 83% yield (480 mg, 0.76 mmol). ^{1}H NMR (300 MHz, [D$_6$]DMSO, 25 °C, TMS): δ = 5.74 (d, ^3J(H,H) = 8.7 Hz, 6H; NH_2), 6.70–6.73 (m, 6H; Ph-H), 7.42–7.48 (m, 6H; Ph-H), 7.54 (d, ^3J(H,H) = 7.2 Hz, 4H; β-pyrrole H), 7.74 (s, 2H; β-pyrrole H), 7.95 ppm (s, 2H; β-pyrrole H); ^{13}C NMR (75 MHz, [D$_6$]DMSO, 25 °C, TMS): δ = 113.95, 114.19, 121.44, 126.65, 127.44, 128.83, 130.08, 132.39, 133.67, 143.27, 144.90, 149.95, 150.54, 150.83, 152.16 ppm; UV/Vis (THF): λ_{max} ($\varepsilon \times 10^{-3}$ L mol^{-1} cm^{-1}) = 387 (186.5), 450 (30.6), 584 (90.5) nm; HRMS (ESI): *m/z*: calcd for $C_{37}H_{26}N_7Cu$: 631.1546; found: 631.1551; elemental analysis (%) calcd for $C_{37}H_{26}N_7Cu$: C 70.29, H 4.15, N 15.51; found: C 70.08, H 3.78, N15.26.

5,10,15-Tris[4-(4-benzylchloride)amidephenyl]corrolatocopper(III) (11): A solution of **10** (100 mg, 0.16 mmol), 4-(chloromethyl)benzoyl chloride (180 mg, 0.95 mmol), and triethylamine (96 mg, 0.95 mmol) was stirred at room temperature for 2 h. After the reaction went to completion, the solvents were evaporated under reduced pressure. The residue was isolated by chromatography on alumina (200—300 mesh) with THF/methanol (200:1). The first fraction was collected. After evaporation of the solvents, the solid was recrystallized from THF/petroleum ether. Compound **11** was obtained as a brown solid in 74% yield (76 mg, 0.07 mmol). ^{1}H NMR (300 MHz, [D$_6$]DMSO, 25 °C, TMS): δ = 4.85 (s, 6H; CH_2), 7.33 (s, 4H; Ph), 7.40 (s, 2H; Ph), 7.59–7.77 (m, 13H; Ph-H and β-pyrrole H), 7.98–8.08 (m, 13H; Ph-H and β-pyrrole H), 10.56 ppm (d, ^3J (H,H) = 6.6 Hz, 3H; NH); ^{13}C NMR (75 MHz, [D$_6$]DMSO, 25 °C, TMS): δ = 46.12, 120.43, 120.68, 128.85, 129.45, 131.37, 135.45, 140.70, 141.83, 166.01 ppm; UV/Vis (THF): λ_{max} ($\varepsilon \times 10^{-3}$ L mol^{-1} cm^{-1}) = 421 (232.2), 541 (25.2) nm; HRMS (ESI): *m/z*: calcd for $C_{61}H_{41}Cl_3N_7CuO_3$: 327.4189; found: 327.4159 $[M^+-3Cl]/3$; elemental analysis (%) calcd for $C_{61}H_{41}Cl_3N_7CuO_3$: C 67.22, H 3.79, N 9.00; found: C 67.51, H 3.56, N 8.99.

5,10,15-Tris[4-(4-*N*-trimethylbenzyl)amidephenyl]corrolatocopper(III) (12): Trimethylamine in alcohol solution (33%, 10 mL) was added to the solution of **11** (35 mg, 0.032 mmol) in THF (10 mL). The reaction mixture was stirred overnight at room temperature. The solvent was evaporated under reduced pressure and the crude product was recrystallized from methanol/petroleum ether. Compound **12** was obtained as a black solid in 98% (40 mg, 0.032 mmol). ^{1}H NMR (300 MHz, [D$_6$]DMSO, 25 °C, TMS): δ = 3.10 (s, 27H; NCH_3), 4.67 (s, 6H; CH_2), 7.77 (s, 16H; Ph-H and β-pyrrole H), 8.06 (s, 8H; Ph-H and β-pyrrole H), 8.19 (d, ^3J (H,H) = 6.0 Hz, 8H; Ph-H and β-pyrrole H), 10.79 ppm (s, 3H; NH); ^{13}C NMR (75 MHz, [D$_6$]DMSO, 25 °C, TMS): δ = 52.65, 67.75, 120.90, 129.02, 132.42, 133.58, 136.98, 165.74 ppm; UV/Vis (CH_3OH): λ_{max} ($\varepsilon \times 10^{-3}$ L mol^{-1} cm^{-1}) = 417 (115.7), 539 (11) nm; HRMS(ESI): *m/z*: calcd for $[C_{70}H_{68}Cl_3N_{10}O_3Cu-3Cl]/3$: 386.4923; found: 386.4923 $[M^+-3Cl]/3$; elemental analysis (%) calcd for $C_{70}H_{68}C_{l3}N_{10}O_3Cu \cdot 3H_2O$: C 63.63, H 5.64, N 10.60; found: C 63.22, H 5.93, N10.14.

5,10,15-Tris[4-(4-*N*-triethylbenzyl)amidephenyl]corrolatocopper(III) (13): A solution of **11** (30 mg, 0.028 mmol) and triethylamine (10 mL, 72 mmol) in THF (10 mL) was stirred and heated to reflux for 16 h. After the solvent and the starting material triethylamine were evaporated under reduced pressure, the crude product was recrystallized from methanol/ether. Compound **13** was obtained as a black solid in 87% yield (33 mg, 0.024 mmol). ^{1}H NMR (300 MHz, [D$_6$]DMSO, 25 °C, TMS): δ = 1.35 (s, 27H; CH_3), 3.25 (s, 18H; NCH_2), 4.61 (s, 6H; CH_2 in benzyl), 7.73 (brs, 16H; Ph-H and β-pyrrole H), 8.18 (brs,16H; Ph-H and β-pyrrole H), 10.79 ppm (brs, 3H; NH); ^{13}C NMR (75 MHz, [D$_6$]DMSO, 25 °C, TMS): δ = 52.75, 59.70, 120.75, 129.09, 131.86, 133.33, 136.96, 165.67 ppm; UV/Vis (CH_3OH): λ_{max} ($\varepsilon \times 10^{-3}$ L mol^{-1} cm^{-1}) = 417 (136.3), 539 (13.2) nm; HRMS (ESI): *m/z*: calcd for $[C_{79}H_{86}Cl_3N_{10}O_3Cu-3Cl]/3$: 428.5393; found: 428.5387 $[M^+-3Cl]/3$; elemental analysis (%) calcd for $C_{79}H_{86}Cl_3N_{10}O_3Cu \cdot 3H_2O$: C 65.55, H 6.41, N 9.68; found: C 65.63, H 6.82, N 9.13.

5,10,15-Tris{4-[4-(1-pyridyl)benzyl]amidephenyl}corrolatocopper(III) (14): This compound was obtained by using the same procedure described for **13**. The starting materials were **11** (40 mg, 0.037 mmol) and pyridine (10 mL, 124 mmol). Compound **14** was obtained as a black solid in 76% yield (37 mg, 0.028 mmol). ^{1}H NMR (300 MHz, [D$_6$]DMSO, 25 °C, TMS): δ = 6.00 (s, 6H; Ph), 7.74 (s, 12H; Ph-H and β-pyrrole H), 8.09 (brs, 13H; Ph-H , pyridine H and β-pyrrole H), 8.24 (s, 8H; pyridine H and β-pyrrole H), 8.68 (s, 6H; pyridine H and β-pyrrole H), 9.30 (s, 8H; pyridine H and β-pyrrole H), 10.69 ppm (s, 3H; NH); ^{13}C NMR (75 MHz, [D$_6$]DMSO, 25 °C, TMS): δ = 63.36, 120.80, 129.26, 129.42, 129.53, 131.73, 136.27, 138.30, 140.66, 145.74, 146.86, 165.80 ppm; UV/Vis (CH_3OH): λ_{max} ($\varepsilon \times 10^{-3}$ L mol^{-1} cm^{-1}) = 417 (126.7), 539 (11.8) nm; HRMS (ESI): *m/z*: calcd for $[C_{76}H_{56}Cl_3N_{10}O_3Cu-3Cl]/3$: 406.4609; found: 406.4606 $[M^+-3Cl]/3$; elemental analysis (%) calcd for $C_{76}H_{56}Cl_3N_{10}O_3Cu \cdot 3H_2O$: C 66.08, H 4.52, N 10.14; found: C 66.02, H 4.89, N 9.75.

5,10,15-Tris{4-[4-*N*-dimethyl-*N*-(2-ethanol]benzyl]amidephenyl}-corrolatocopper(III) (15): This compound was obtained by using the same procedure described for **13**. The starting materials were **11** (40 mg, 0.037 mmol) and 2-(dimethylamino)ethanol (10 mL, 100 mmol). Compound **15** was obtained as a black solid in 84% yield (42 mg, 0.031 mmol). ^{1}H NMR (300 MHz, [D$_6$]DMSO, 25 °C, TMS): δ = 3.06 (s,

18H; NCH_3), 3.94 (s, 6H; NCH_2), 4.71 (s, 6H; CH_2 in ethanol), 5.50 (s, 6H; CH_2), 7.80 (s, 13H; Ph-H), 8.03 (br s, 6H; Ph-H and β-pyrrole H), 8.15 (br s, 13H; Ph-H and β-pyrrole H), 10.72 ppm (br s, 3H; NH); ^{13}C NMR (75 MHz, [D_6]DMSO, 25 °C, TMS): $\delta = 50.77$, 55.60, 66.02, 67.44, 120.80, 128.93, 132.17, 133.87, 136.99, 165.74 ppm; UV/Vis (CH_3OH): λ_{max} ($\varepsilon \times 10^{-3}$ L mol^{-1} cm^{-1}) = 417 (134.7), 539 (12.4) nm; HRMS (ESI): m/z: calcd for [$C_{73}H_{74}Cl_3N_{10}O_3Cu-3Cl$]/3: 416.5029; found: 416.5026 [M^+-3Cl]/3; elemental analysis (%) calcd for $C_{73}H_{74}Cl_3N_{10}O_3Cu \cdot 3H_2O$: C 62.12, H 5.71, N 9.92; found: C 61.75, H 6.11, N 9.61.

Biology

Materials: All the oligomers/primers were synthesized and PAGE purified by Invitrogen Technology (Shanghai, China). Taq DNA polymerase was purchased from Toyobo (China). CT-DNA was purchased from Biosharp (China). The oligomers Pu27 (5′-TGGGGAGGGTGGGGAGGGTGGGGAAGG-3′), Pu27 mu (5′-TGGGGAGGGTGGAAAGGGTGGGGAAGG-3′), and RevPu27 (5′-ATCGATCGCTTCTCGTCCTTCCCCA-3′) were used in the PCR stop assay, the sequence Telo24 (5′-TTAGGGTTAGGGTTAGGGTTAGGG-3′) was used in CD spectroscopy, and G4C (5′-CATGG TGGTTT GGGTTA GGGTTA GGGTTA GGGTTA CCAC-3′) was used in CD melting. The sequence G4A (5′-AGGGTTAGGGTTAGGGTTAGGG-3′) was used in the UV/Vis titration experiments.

PCR stop assay: The PCR stop assay performed was different from the previous study. The test oligomers 21G, 21Gmu or Pu27, Pu27 mu and the corresponding complementary sequences Rev21G and RevPu27 were used in the current study.[23,26] The reactions were performed in 1×PCR buffer, containing a mixture of 21G, Rev21G, dNTP, Taq polymerase, and the corresponding corrole derivatives in solution with water and were amplified by PCR at a total volume of 12.5 μL. After PCR, 2 μL of loading buffer (solution (10 mL) included glycerol (1 mL), bromophenol blue (25 mg), and Ficoll-400 (1.5 g)) was added to each mixture. The samples were subsequently analyzed by 16% nondenaturing polyacrylamide gels, which were carried out in 1×Tris/borate/EDTA buffers at room temperature. The gels were stained by using ethidium bromide and photos were taken.[23–26]

CD spectroscopy: The CD experiments, utilizing a Jasco-810 spectropolarimeter (Jasco, Easton, MD, USA), were measured at room temperature using a quartz cell with a 1-mm path length cuvette. The CD spectra were collected at $\lambda = 220$–350 nm with a scanning speed of 100 nm min^{-1}. The oligomer d(T_2AG_3)$_4$, at a final concentration of 12.5 μM, was resuspended in 10 mM Tris–HCl buffer (1 mM EDTA, pH 7.4) in the absence or presence of 100 mM NaCl. Various amounts of a stock solution of the corrole were continually added to increase the concentration ratio of corrole/DNA strand. All the CD spectra were baseline corrected for signal contributions from the buffer.[8,30]

CD thermal melting studies: A solution of G4C oligomer (10 μM; sequence 5′-CATGGTGGTTTGGGTTAGGGTTAGGGTTAGGGTTACCAC-3′) was prepared in Na^+ buffer (10 mM Tris–HCl, 1 mM EDTA, 100 mM NaCl, pH 7.4) containing 50 μM corrole to be tested, the mixture was first heated to 95 °C for 5 min, then slowly cooled to room temperature, and incubated at 4 °C for at least 6 h. The CD spectra were recorded on a Jasco-810 spectropolarimeter equipped with a temperature controller with a response time of 1 s and a bandwidth of 1 nm. The CD melting curves were obtained by monitoring the absorbance at $\lambda = 295$ nm while the temperature was increased from 20 to 85 °C at about 1.5 °C min^{-1}.[6b,8,30]

SPR testing: The oligonucleotides and materials purchased from Sangon (Shanghai, China) are G4 quadruplex: 5′-biotin-$AG_3(TTAG_3)_3$-3′; DNA duplex: 5′-biotin-GGGCATAGTGCGTGGGCGTTAGC-3′; complementary strand: (5′-TAACGCCCACGCACTATGCC-3′).

Immobilization of the DNA and SPR binding: Biotinylated DNA was immobilized on a CM5 sensor chip (BIAcore, Switzerland) with streptavidin by using a BIAcore 3000 optical biosensor. Streptavidin was coupled to the carboxymethylated dextran matrix covering the surface of the sensor chip by using an amine coupling kit (BIAcore, Switzerland) according to the manufacturer's instruction. Biotinylated oligonucleotide (0.5 μM) in coupling buffer (10 mM Tris, pH 7.4, 1 mM EDTA, and 150 mM LiCl) was heated at 95 °C for 5 min and cooled slowly to room temperature. Then biotin–DNA (30 μL) was injected at a flow rate of 5 μL min^{-1}. One of the flow cells was used to immobilize the DNA and another served as a blank reference.

All the samples were dissolved in dimethylsulfoxide (DMSO; 10 mM) and prepared in freshly filtered and degassed running buffer (*N*-(2-hydroxyethyl)-piperazine-*N*′-2-ethanesulfonic acid (HEPES) buffer saline HBS–EP/KCl, pH 7.4, 0.01 M HEPES, 0.2 M KCl, 3 mM EDTA, and 0.005% (v/v) surfactant P20) by serial dilutions from stock solutions. This DNA folded in the running buffer with K^+ ions (200 mM) and formed a quadruplex during extended flow in the SPR experiments.[31]

The dsDNA consisted of biotin–oligoDNA hybridized with its complementary sequence. The sensor chip was regenerated by injection of NaOH/NaCl (20 mM/1 M, 5 μL). All the procedures used repetitive cycles of the same injection and regeneration.

DNA binding experiments were carried out in the running buffer (pH 7.4, 0.01 M HEPES, 0.2 M KCl, 3 mM EDTA, and 0.005% (v/v) surfactant P20) at a flow rate of 10 mL min^{-1}.

Fitting of the kinetic data: Generally kinetics parameters are obtained by global fitting of the kinetic data by using the BIAevaluation program with 1:1 binding with mass transfer. The values k_a and k_d are the corresponding association and dissociation rate constants: $K_A = k_a/k_d$ and $K_D = k_d/k_a$.[8,31]

UV/Vis titration assay: The corroles were prepared in a solution of DMSO (10 mM). G4A was dissolved in 10 mM Tris—HCl, 1 mM EDTA, and 100 mM NaCl to form a 100 μM solution with respect to G4A. The solution was heated at 95 °C for 5 min, cooled down to room temperature, and stored in the refrigerator. CT-DNA was dissolved in 10 mM Tris—HCl and 1 mM EDTA. The concentration of CT-DNA was determined by measuring the absorbance at $\lambda = 260$ nm with an extinction coefficient of 13 100 M^{-1} cm^{-1}.

The absorption spectra were collected at room temperature using a Shimadzu 1901 UV/Vis double-beam spectrophotometer. Quartz cuvettes with a path length of 1 cm were used for all the absorbance studies. A solution of 10 mM Tris—HCl, 1 mM EDTA, and 100 mM NaCl at pH 7.4 was used for the G4A DNA and a solution of 10 mM Tris—HCl and 1 mM EDTA at pH 7.4 was used for the CT-DNA.

All the absorption titrations were performed by adding a stock solution of G4A in 10 mM Tris—HCl, 1 mM EDTA, and 100 mM NaCl at pH 7.4 to a cuvette containing some corroles in 10 mM Tris—HCl, 1 mM EDTA, and 100 mM NaCl at pH 7.4 (see Figure S4 in the Supporting Information). For the CT-DNA, the titrations were performed by adding a stock solution of CT-DNA in 10 mM Tris—HCl and 1 mM EDTA at pH 7.4 to a cuvette containing some corroles in 10 mM Tris—HCl and 1 mM EDTA at pH 7.4 (see Figure S5 in the Supporting Information).

Acknowledgements

This work was supported by the National Science of Foundation of China (No. 20672084), National Science Fund for Distinguished Young Scholars (No. 20425206), the Cultivation Fund of the Key Scientific and Technical Innovation Project, the Ministry of Education of China (No. 706040), the State Key Laboratory of Natural and Biomimetic Drugs, and the State Key Laboratory of Applied Organic Chemistry.

[1] a) J. L. Sessler, S. J. Weghorn, *Expanded, Contracted, and Isomeric Porphyrins*, Pergamon, Oxford, **1997**, pp. 11–125; b) A. Jasat, D. Dolphin, *Chem. Rev.* **1997**, *97*, 2267–2340.
[2] a) R. Grigg, R. J. Hamilton, M. L. Josefowicz, C. H. Rochester, R. T. Terrell, H. Wickwar, *J. Chem. Soc. Perkin Trans. 2* **1973**, 407–413; b) A. W. Johnson, I. T. Kay, *J. Chem. Soc.* **1965**, 1620–1629.
[3] Z. Gross, H. B Gray, *Comments Inorg. Chem.* **2006**, 27, 61–72.

[4] a) L. R. Kelland, *Eur. J. Cancer* **2005**, *41*, 971–979; b) J. L. Mergny, J. F. Riou, P. Mailliet, M. P. Teulade-Fichou, E. Gilson, *Nucleic Acids Res.* **2002**, *30*, 839–865.
[5] a) Y. Wang, D. J. Patel, *Structure* **1993**, 1, 263–282; b) A. T. Phan, V. Kuryavyi, K. N. Luu, D. J. Patel, *Proc. Natl. Acad. Sci. USA* **2007**, 35, 4927–4940; c) J. X. Dai, C. Punchihewa, A. Ambrus, D. Chen, R. A. Jones, D. Z. Yang, *Proc. Natl. Acad. Sci. USA* **2007**, *104*, 2440–2450; d) A. Ambrus, D. Chen, J. X. Dai, T. Bialis, R. A. Jones, D. Z. Yang, *Proc. Natl. Acad. Sci. USA* **2006**, *103*, 2723–2735; e) E. M. Rezler, J. Seenisamy, S. Bashyam, M. Y. Kim, E. White, W. D. Wilson, L. H. Hurley, *J. Am. Chem. Soc.* **2005**, *127*, 9439–9447.
[6] a) V. Gabelica, E. S. Baker, M. P. Teulade-Fichou, E. De Pauw, M. T. Bowers, *J. Am. Chem. Soc.* **2007**, *129*, 895–904; b) L. G. Ren, A. M. Zhang, J. Huang, P. Wang, X. C. Weng, L. X. Zhang, F. Liang, Z. Tan, X. Zhou, *ChemBioChem* **2007**, *8*, 775–780; c) E. S. Baker, J. T. Lee, J. L. Sessler, M. T. Bowers, *J. Am. Chem. Soc.* **2006**, *128*, 2641–2648; d) J. F. Riou, *Curr. Cancer Drug Targets* **2004**, *4*, 439–443; e) R. T. Wheelhouse, D. Sun, H. Han, F. X. Han, L. H. Hurley, *J. Am. Chem. Soc.* **1998**, *120*, 3261–3262; f) N. V. Anantha, M. Azam, R. D. Sheardy, *Biochemistry* **1998**, *37*, 2709–2714.
[7] Z. Gershman, I. Goldberg, Z. Gross, *Angew. Chem.* **2007**, *119*, 4398–4402; *Angew. Chem. Int. Ed.* **2007**, *46*, 4320–4324.
[8] B. Q. Fu, J. Huang, L. G. Ren, X. C. Weng, Y. Y. Zhou, Y. H. Du, X. J. Wu, X. Zhou, G. F. Yang, *Chem. Commun.* **2007**, 3264–3266.
[9] J. E. Reed, A. A. Amal, S. Neidle, R. Vilar, *J. Am. Chem. Soc.* **2006**, *128*, 5992–5993.
[10] P. J. Perry, M. A. Read, R. T. Davies, S. M. Gowan, A. P. Reszka, A. A. Wood, L. R. Kelland, S. Neidle, *J. Med. Chem.* **1999**, *42*, 2679–2684.
[11] R. J. Harrison, J. Cuesta, G. Chessari, M. A. Read, . S. K. Basra, A. P. Reszka, J. Morrell, S. M. Gowan, C. M. Incles, F. A. Tanious, W. D. Wilson, . L. R. Kelland, S. Neidle, *J. Med. Chem.* **2003**, *46*, 4463–4476.
[12] K. Jantos, R. Rodriguez, S. Ladame, P. S. Shirude, S. Balasubramanian, *J. Am. Chem. Soc.* **2006**, *128*, 13662- 13663.
[13] P. S. Shirude, E. R. Gillies, S. Ladame, F. Godde, K. Shin-ya, I. Huc, S. Balasubramanian, *J. Am. Chem. Soc.* **2007**, *129*, 11890–11891.
[14] A. D. Moorhouse, A. M. Santos, M. Gunaratnam, M. Moore, S. Neidle, J. E. Moses, *J. Am. Chem. Soc.* **2006**, *128*, 15972–15973.
[15] A. D. Cian, E. DeLemos, J.-L. Mergny, M.-P. Teulade-Fichou, D. Monchaud, *J. Am. Chem. Soc.* **2007**, *129*, 1856–1857.
[16] I. M. Dixon, F. Lopez, A. M. Tejera, J.-P. Estève, M. A. Blasco, G. Pratviel, B. Meunier, *J. Am. Chem. Soc.* **2007**, *129*, 1502–1503.
[17] K. Nemoto, Y. Kondo, S. Himeno, Y. Suzuki, S. Hara, M. Akimoto, N. Imura, *Biochem. Pharmacol.* **2000**, 59, 401–405.
[18] I. H. Wasbotten, T. Wondimagegn, A. Ghosh, *J. Am. Chem. Soc.* **2002**, *124*, 8104.
[19] M. Read, R. J. Harrison, B. Romagnoli, F. A. Tanious, S. H. Gowan, A. P. Reszka, W. D. Wilson, L. R. Kelland, S. Neidle, *Proc. Natl. Acad. Sci. USA* **2001**, *98*, 4844–4849.
[20] S. Nardis, D. Monti, R. Paolesse, *Mini-Rev. Org. Chem.* **2005**, *2*, 355–374.
[21] a) D. S. Sigman, *Acc. Chem. Res.* **1986**, *19*, 180–186; b) D. S. Sigman, A. Mazunder, D. M. Perrin, *Chem. Rev.* **1993**, *93*, 2295–2316; c) P. U. Maheswari, S. Roy, H. den Dulk, S. Barends, G. van Wezel, B. Kozlevcar, P. Gamez, J. Reedijk, *J. Am. Chem. Soc.* **2006**, *128*, 710–711.
[22] a) I. H. Wasbotten, T. Wondimagegn, A. Ghosh, *J. Am. Chem. Soc.* **2002**, *124*, 8104–8116; b) C. Bru1ckner, R. P. Brinas, J. A. K. Bauer, *Inorg. Chem.* **2003**, *42*, 4495–4497; c) I. Aviva, Z. Gross, *Chem. Commun.* **2007**, 1987–1999.
[23] T. Lemarteleur, D. Gomez, R. Paterski, E. Mandine, P. Mailliet, J. F. Riou, *Biochem. Biophys. Res. Commun.* **2004**, *323*, 802–808.
[24] P. Balagurumoorthy, S. K. Brahmachari, *J. Biol. Chem.* **1994**, *269*, 21858–21869.
[25] P. Balagurumoorthy, S. K. Brahmachari, D. Mohanty, M. Bansal, V. Sasisekharan, *Nucleic Acids Res.* **1992**, *20*, 4061–4067.
[26] T. M. Ou, Y. J. Lu, C. Zhang, Z. S. Huang, X. D. Wang, J. H. Tang, Y. Chen, D. L. Ma, K. Y. Wong, J. C. Tang, A. S. Chan, L. Q. Gu, *J. Med. Chem.* **2007**, *50*, 1465–1474.
[27] C. L. Grand, T. J. Powell, R. B. Nagle, D. J. Bearss, D. Tye, M. Gleason-Guzman, L. H. Hurley, *Proc. Natl. Acad. Sci. USA* **2004**, *101*, 6140–6145.
[28] a) I. M. Dixon, F. Lopez, A. M. Tejera, J.-P. Estè ve, M. A. Blasco, G. Pratviel, B. Meunier, *J. Am. Chem. Soc.* **2007**, *129*, 1502–1503; b) J. Bendix, H. B. Gray, G. Golubkov, Z. Gross, *Chem Commun.* **2000**, 1957–1958.
[29] R. Giraldo, M. Suzuki, L. Chapman, D. Rhodes, *Proc. Natl. Acad. Sci. USA* **1994**, *91*, 7658–7662.
[30] D. P. N. Goncalves, R. Rodriguez, S. Balasubramanian, J. K. M. Sanders, *Chem. Commun.* **2006**, 4685–4687.
[31] P. Wang, L. Ren, H. He, F. Liang, X. Zhou, Z. Tan, *ChemBioChem* **2006**, *7*, 1155–1159.
[32] J. E. Reed, A. A. Arnal, S. Neidle, R. Vilar, *J. Am. Chem. Soc.* 2006, 128, 5992–5993.
[33] L. R. Keating, V. A. Szalai, *Biochemistry* **2004**, *43*, 15891–15900.
[34] R. F. Pasternack, E. J. Gibbs, J. J. Villafranca, *Biochemistry* **1983**, *22*, 2406–2414.

Received: May 2, 2008
Published online: August 27, 2008

